

DynaBARN: Benchmarking Metric Ground Navigation in Dynamic Environments

Anirudh Nair¹, Fulin Jiang¹, Kang Hou¹, Zifan Xu¹, Shuoze Li¹, Xuesu Xiao^{2,3}, and Peter Stone^{1,4}

Abstract—Safely avoiding dynamic obstacles while moving toward a goal is a fundamental capability of autonomous mobile robots. Current benchmarks for dynamic obstacle avoidance do not provide a way to alter how obstacles move and instead use only a single method to uniquely determine the movement of obstacles, e.g., constant velocity, the social force model, or Optimal Reciprocal Collision Avoidance (ORCA). Using a single method in this way restricts the variety of scenarios in which the robot navigation system is trained and/or evaluated, thus limiting its robustness to dynamic obstacles of different speeds, trajectory smoothness, acceleration/deceleration, etc., which we call *motion profiles*. In this paper, we present a simulation testbed, DynaBARN, to evaluate a robot navigation system’s ability to navigate in environments with obstacles with different motion profiles, which are systematically generated by a set of difficulty metrics. Additionally, we provide a demonstration collection pipeline that records robot navigation trials controlled by human users to compare with autonomous navigation performance and to develop navigation systems using learning from demonstration. Finally, we provide results of four classical and learning-based navigation systems in DynaBARN, which can serve as baselines for future studies. We release DynaBARN open source as a standardized benchmark for future autonomous navigation research in environments with different dynamic obstacles. The code and environments are released at <https://github.com/aninair1905/DynaBARN>.

I. INTRODUCTION

With autonomous mobile robots being deployed in the real world, such as for package delivery on crowded sidewalks, autonomous driving in dense traffic, and intelligent warehouses with hundreds of moving objects, safely avoiding dynamic obstacles in the environment while efficiently reaching their goal is now a fundamental robot capability. Navigation among dynamic obstacles has been studied for decades, especially in the domain of multi-agent path planning [1], [2] and autonomous driving [3], [4]. More recently, machine learning techniques for dynamic obstacle avoidance have been applied to multi-robot systems [5], [6] and social navigation [7]–[9].

Despite the abundance of research in navigation with dynamic obstacle avoidance, there is no generally accepted metric by which to compare methods against each other.

While difficulty in navigating in a static environment is relatively easy to quantify [10], there are more factors to consider with dynamic obstacles such as obstacles’ speed, direction, acceleration/deceleration, smoothness, etc. However, existing simulation environments to develop and test dynamic obstacle avoidance methods typically only contain obstacles that move using a single method, such as constant velocity, the social force model [11], or Optimal Reciprocal Collision Avoidance (ORCA) [12]. As a result, the obstacles in such simulation environments have similar motion profiles (i.e., speed, direction, acceleration/deceleration, smoothness, etc.) and only the navigation system’s ability to avoid such obstacles is tested, ignoring its robustness to obstacles with other motion profiles. Considering that dynamic obstacles in the real world do not necessarily always follow one single motion profile (e.g., a pedestrian and a scooter may move differently on a sidewalk around a delivery robot), a good dynamic obstacle avoidance method should be able to avoid obstacles with different motion profiles.

To address the lack of a standardized method to compare and test mobile robot navigation in dynamic environments containing obstacles with varying motion profiles, we introduce DynaBARN. DynaBARN is an extension to the Benchmark Autonomous Robot Navigation (BARN) dataset of 300 simulated, static, highly constrained navigation environments [10] with 300 environments containing dynamic obstacles with different motion profiles. These environments are generated to cover a wide variety of obstacle motion profiles of different navigation difficulties, which are systematically quantified by a set of difficulty metrics. We develop a data collection pipeline that records navigation trials performed by human teleoperators, to provide a reference of human performance at dynamic obstacle avoidance. The resulting training data may also be useful for developing learning-based navigation systems. Finally, we provide results of four classical and learning-based navigation systems in DynaBARN, including Dynamic Window Approach (DWA) [13], Timed Elastic Band (TEB) [14], a reinforcement learning approach [15], and a vanilla behavioral cloning method using human demonstrations collected from the pipeline we provide [16], which can serve as baselines for future studies. In summary, this paper makes the following contributions.

- A benchmark dataset (DynaBARN) of 300 pre-generated dynamic environments in simulation for metric ground navigation, along with an environment generation procedure to generate new dynamic environments,
- A data collection pipeline to collect human-demonstrated navigation trials in the simulated

¹Department of Computer Science, The University of Texas at Austin ²Department of Computer Science, George Mason University ³Everday Robots ⁴Sony AI {ani.nair, fj3279, kevinhou, zfxu, shuoze.li}@utexas.edu, xiao@gmu.edu, pstone@cs.utexas.edu

This work has taken place in the Learning Agents Research Group (LARG) at UT Austin. LARG research is supported in part by NSF (CPS-1739964, IIS-1724157, NRI-1925082), ONR (N00014-18-2243), FLI (RFP2-000), ARO (W911NF-19-2-0333), DARPA, Lockheed Martin, GM, and Bosch. Peter Stone serves as the Executive Director of Sony AI America and receives financial compensation for this work. The terms of this arrangement have been reviewed and approved by the University of Texas at Austin in accordance with its policy on objectivity in research.

environments,

- Baseline results from a set of existing navigation systems in DynaBARN.

II. RELATED WORK

In this section, we discuss existing navigation methods in dynamic environments as well as testbeds for dynamic obstacle avoidance.

A. Navigation in Dynamic Environments

Robotics researchers have investigated methods for dynamic obstacle avoidance for decades. The social force model [17] determines a pedestrian’s motion influenced by the motion of other pedestrians as well as social groups. In contrast, ORCA [12] and RVO [18] are reactive methods for crowded navigation where each agent takes a share of the responsibility for avoiding pairwise collisions and assumes the other agents will reciprocate.

More recently, learning based approaches for dynamic obstacle avoidance have emerged [19]. CADRL [20] uses Deep Reinforcement Learning (DRL) for collision avoidance; it has been extended to include socially-aware collision avoidance [21] by inducing social norms such as passing on the right, overtaking, and crossing. Moreover, DRL dynamic obstacle avoidance methods have been used with conventional waypoint generators so they can be used in conventional navigation systems [22]. The ability to guide or follow a human has also been incorporated into dynamic obstacle avoidance methods for assistive robotics [23]. In addition to DRL methods, inverse reinforcement learning has also been used for socially compliant robot navigation among pedestrians by modeling human behaviors in terms of a mixture distribution that captures both the discrete navigation decisions, such as going left or right, as well as the natural variance of human trajectories [24].

B. Testbeds for Dynamic Obstacle Avoidance

While testbeds for navigation and obstacle avoidance [10], [25], [26] in static environments [27]–[34] have been used to benchmark research progress, simulation testbeds for dynamic obstacle avoidance have recently been of interest in the research community.

For social navigation around humans, Pedsim [35] simulates crowds of pedestrians and incorporates methods of individual and group behaviors into an environment. Pedsim does not incorporate social scenarios into its model. As a result, many subsequent simulation testbeds, such as SEAN 2.0 [36], Arena-Bench [37], and SocNavBench [38], use the social forces model along with Pedsim to simulate social scenarios and interactions. However, all pedestrians (obstacles) in the aforementioned simulators have similar motion profiles. For instance, in Arena-Bench, the obstacle speeds are set to a constant 0.3m/s, and in SEAN 2.0 when the pedestrians move, they move at a constant 1.4m/s. These testbeds do not incorporate obstacles that have different motion profiles, whereas in reality, a robot must be able to avoid colliding with dynamic obstacles moving at different speeds and with path irregularities. Consider the fact that slowly walking pedestrians and fast swerving scooters may appear

at the same time on a sidewalk; or at a busy intersection, cars, motorcycles, bicycles, pedestrians, or pets may move in completely different manners. DynaBARN contains obstacles moving not only at different speeds, but also changing speeds between waypoints to test a navigation system’s robustness to erratic changes. These changes in speed and trajectory are tunable based on a set of intuitive difficulty metrics.

Multi-agent path planning testbeds are also used for CADRL [20] and its socially aware counterpart [21]. However, these testbeds aim at testing multi-agent systems in which each agent learns to navigate while avoiding collisions with the other agents: the agents’ policies are trained together in the same simulation to create one shared policy. DynaBARN does not feature multi-agent path planning, in the sense that dynamic obstacles are not treated as agents, which will react to the robot and other obstacles. Instead, the obstacles’ motions are predetermined by waypoints and it is the navigation system’s responsibility to robustly avoid collisions with obstacles of a variety of motion profiles.

III. APPROACH

In this section, we describe our method of creating the DynaBARN environments. In Sec. III-A, we describe the way the obstacle trajectories are generated from user-specified metrics. In Sec. III-B, we describe how to create environments from the generated obstacle trajectories. In Sec. III-C, we introduce a method to quantify the difficulty of an environment in DynaBARN. In Sec. III-D, we describe the human demonstration collection pipeline.

A. Obstacle Trajectory Generation

Motion profiles for the obstacles are the trajectories represented by multiple waypoints, each of which contains two values: the position and timestamp of the obstacle. Formally, we define a trajectory for an obstacle as a sequence of waypoints $\langle c_i \rangle_{i=0}^N$ with $c_i = ((x_i, y_i), t_i)$, where (x_i, y_i) is the coordinate point and t_i is the timestamp of the obstacle at that coordinate point. We assume all obstacles are cylindrical with the base parallel to the ground and therefore ignore their orientation for simplicity. In this work, the environment is a 20×20 meter grid world. The trajectories are generated using a polynomial function that is fit to randomly sampled points within the grid. The number of randomly sampled points depends on the order of the polynomial. More specifically, $n + 1$ randomly sampled points determine the equation of a polynomial of degree n . Thus, from a range of orders given by the user, order_{\min} and order_{\max} as the minimum and the maximum orders respectively, the method samples a random order n and randomly samples $n + 1$ points from the $[-10, 10] \times [-10, 10]$ grid. A trajectory generated by a lower degree polynomial will be smoother resembling a straighter line than a trajectory made from a higher degree polynomial, which will look less smooth and more erratic. Once the polynomial is fit to the randomly-sampled points, the method then calculates the (x_i, y_i) coordinate points at every integer x -value in $[-10, 10]$ using the polynomial and then puts them into an array c . The method then takes the coordinate points where the polynomial intersects the edges

of the 20×20 grid and appends them to the array c . Any points in c outside of the 20×20 grid as a result of the polynomial fitting are removed. The array c is then, with equal probabilities, sorted either descendingly or ascendingly with respect to the x -values. This random sorting avoids the bias towards environments that only have obstacles move in one direction. We use a straight line to approximate the movement between two points. Examples of trajectories 3-degree polynomials are shown in Fig. 1.

Next, the method creates the timestamp at which the obstacle reaches each waypoint. The first point in c is assigned the time 0 seconds since it is the starting waypoint. For each subsequent coordinate point in c , the distance d between the current point c_i and the previous coordinate point c_{i-1} is calculated. The method then samples the speed (meters per second) $s \sim \mathcal{N}(\text{avg_speed}, \text{avg_std}^2)$ from c_{i-1} to c_i , where $\text{avg_speed} \sim \mathcal{U}\{\text{speed}_{\min}, \text{speed}_{\max}\}$ and $\text{avg_std} \sim \mathcal{U}\{\text{std}_{\min}, \text{std}_{\max}\}$. \mathcal{N} is a normal distribution parameterized by mean avg_speed and variance avg_std^2 , and \mathcal{U} is a continuous uniform distribution. The parameters speed_{\min} , speed_{\max} , std_{\max} , and std_{\min} are all given by the user. A trajectory with a high standard deviation will cause less predictable changes in speed from waypoint to waypoint. Additionally, the speed is limited below by speed_{\min} and above by speed_{\max} . Once s is sampled, the time taken by an obstacle to travel from c_{i-1} to c_i can be computed as $\Delta t_i = \frac{d}{s}$. The timestamp of the next waypoint can, therefore, be computed recursively by $t_i = t_{i-1} + \Delta t_i$ to get the overall time at which the obstacles will reach (x_i, y_i) . We can then create a trajectory for an obstacle composed of a sequence of waypoints $\langle c_i \rangle_{i=0}^N$ in which each waypoint has a position and a timestamp which the obstacle reaches said position. The trajectory generation process is shown in Alg. 1

B. Environment Generation

To generate an environment in DynaBARN, the user inputs obstacles_{\max} and obstacles_{\min} which are the maximum and minimum numbers of obstacles, respectively, for the environment. Then for each obstacle, a trajectory of waypoints is created using the method described in Sec. III-A. The result is a list of trajectories, one for each obstacle.

C. Difficulty

a) Motion Profile Difficulty: We provide a method to quantify the difficulty of each environment in DynaBARN. There are 6 parameters that can be set for each obstacle in DynaBARN as described in Sec. III-A: the maximum and minimum for each of speed (speed_{\max} and speed_{\min}), standard deviation of speed between waypoints (std_{\max} and std_{\min}), and order (order_{\max} and order_{\min}). An obstacle with a higher average speed will be more difficult for a robot to react to compared to one with a lower average speed. Similarly, it is more difficult for a navigation system to avoid colliding with an obstacle with a larger standard deviation rather than one with a smaller one. For instance, with a high standard deviation, an obstacle can change between high and low speeds from waypoint to waypoint, making its motion relatively unpredictable for a robot navigation

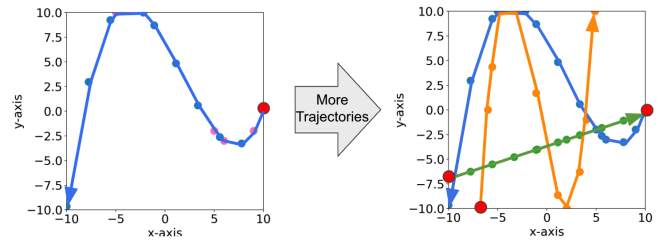


Fig. 1: An example of the process of creating coordinate points and trajectories. The pink points in the top graph resemble the points used to fit the 3-degree polynomial. Then, the remaining coordinate points at every whole number x -values from $[-10, 10]$, as shown by the blue points in the top graph, are calculated using the polynomial. Using these points, the trajectory for the obstacle is created, as shown by the blue line. Similarly, more obstacle trajectories are created in the bottom graph.

Algorithm 1 Obstacle Trajectory Generation

Require: $\text{speed}_{\max}, \text{speed}_{\min}, \text{order}_{\max}, \text{order}_{\min}, \text{std}_{\max}, \text{std}_{\min}$

- 1: $n_{\text{order}} \sim \mathcal{U}\{\text{order}_{\min}, \text{order}_{\max}\}$
- 2: Generate $n_{\text{order}} + 1$ points in $[-10, 10] \times [-10, 10]$
- 3: Fit polynomial p with $n_{\text{order}} + 1$ points
- 4: Calculate the (x_i, y_i) coordinate points at every integer x -value in $[-10, 10]$ using p
- 5: Calculate where the p intersects the edges of the $[-10, 10] \times [-10, 10]$ grid and append them to $\langle c_i \rangle_{i=0}^N$
- 6: Sort c from either highest to lowest or lowest to highest x -value
- 7: $t_0 = 0$ seconds
- 8: **for** c_i starting at $i = 1$ **do**
- 9: $d \leftarrow$ distance from (x_{i-1}, y_{i-1}) to (x_i, y_i)
- 10: $\text{avg_speed} \sim \mathcal{U}\{\text{speed}_{\min}, \text{speed}_{\max}\}$
- 11: $\text{avg_std} \sim \mathcal{U}\{\text{std}_{\max}, \text{std}_{\min}\}$
- 12: $s \sim \mathcal{N}(\text{avg_speed}, \text{avg_std}^2)$
- 13: $t_i \leftarrow \frac{d}{s} + t_{i-1}$
- 14: **end for**
- 15: **return** $\langle c_i \rangle_{i=0}^N$

system. Moreover, a trajectory based on a higher order polynomial will have a less straightforward path and will also be less predictable to a robot navigation system. Using these parameters, we can select ranges that divide an obstacle's motion profiles into two categories: easy and hard. Based on the Jackal robot which we use to conduct navigation tasks (see Sec. IV for specifications), a categorization of the motion profiles of the obstacles can be designed as shown in Table I. These motion profiles can be changed based on the user's preferences.

b) Overall Environment Difficulty: The amount of obstacles in an environment can also affect difficulty, as shown in [37]. An increased number of obstacles will naturally make the environment more difficult to navigate, and an environment with many obstacles that have a hard motion profile will be even more difficult. To determine difficulty, we

Algorithm 2 Environment Generation

Require: $obstacle_number_{max}, obstacle_number_{min}$
1: $obstacle_number \sim \mathcal{U}\{obstacles_{min}, obstacles_{max}\}$
2: **for** obstacle in $obstacle_number$ **do**
3: Create trajectory with Alg. 1
4: **end for**
5: **return** List of trajectories

TABLE I: Easy and Hard Obstacle Motion Profiles

	Easy	Hard
$[order_{min}, order_{max}]$	[1, 2]	[3, 4]
$[speed_{min}, speed_{max}]$	[0.5, 1.0]	[1.0, 2.0]
$[std_{min}, std_{max}]$	[0.01, 0.1]	[0.1, 0.2]

first choose the number of obstacles for an environment and then choose the motion profiles for the obstacles. A lower number of obstacles with easy motion profiles will result in easy difficulty while a lower number of obstacles but hard motion profiles will result in medium difficulty. Similarly, an environment with a high number of obstacles with easy motion profiles will also result in medium difficulty, but an environment with both high number of obstacles and hard motion profiles will result in a hard environment difficulty. Fig 2 shows a tree-diagram for determining the difficulty.

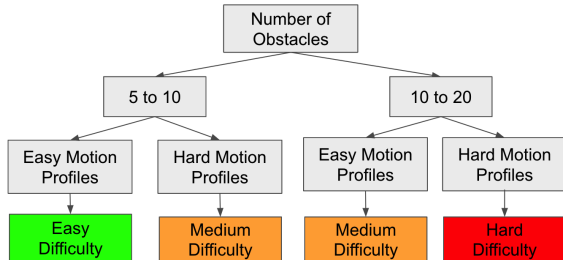


Fig. 2: Diagram for determining environment difficulty.

D. Human Demonstration Collection

We develop a human demonstration data collection pipeline for future researchers to collect human demonstrations of navigation behaviors in dynamic obstacle environments.¹ Our open-sourced data collection pipeline automatically sets up the ROS environment and installs the required packages for running a simulated unmanned ground vehicle, a Clearpath Jackal, in Gazebo simulation. After finishing the setup, users will be prompted to choose an environment number to open the corresponding dynamic environment. After the selection, Gazebo will be launched and a Jackal will be spawned at (0.0, 11.0), while the navigation goal is set to (0.0, -9). The user will need to drive through the moving obstacles (red cylinders in Fig 3) and try to reach the goal (the green dot in Fig 3) using a joystick. When the Jackal reaches the goal, Gazebo will stop and exit. The human demonstration data is recorded as ROS bag files [39] saved in the local folder. In the ROS bag file, all topics relevant

¹Link to the Human Demonstration Collection pipeline repository is at <https://github.com/kevinhou912/ROS-Jackal-Data-Collection-Local.git>

to navigation have been recorded, including `front/scan`, `cmd_vel`, and other `move_base` related topics, which can be used to train an imitation learning policy. The human demonstration pipeline can be extended to any Gazebo world, such as the static BARN environments [10], as long as the world has a goal object. While future researchers can use our

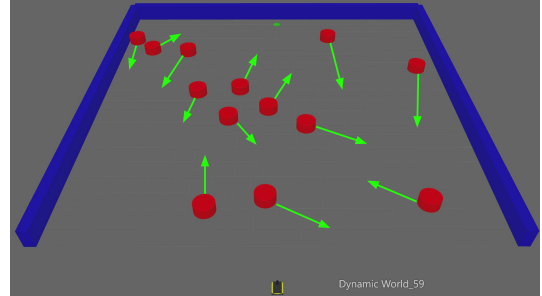


Fig. 3: An example of a world in DynaBARN. The Jackal robot has a dimension of 500 x 430 x 250 mm (L x W x H) and a maximum speed of 2 m/s while the radius of our cylinder obstacles is 0.5 m. Jackal spawns at the bottom of the figure and is given the objective to reach the goal at the top shown by the green point while not colliding into the red obstacles. The green lines indicate the trajectory of the obstacles to their next respective waypoint.

pipeline to collect navigation demonstration data collection from a wider variety of human experts, for ease of use, we provide 60 demonstration trials for DynaBARN from two co-authors of the paper.

IV. EXPERIMENTS AND RESULTS

In this section, we implement and benchmark four commonly-used baselines for dynamic obstacle avoidance tasks using DynaBARN. We sample 60 environments out of the 300 generated worlds in DynaBARN to use for our baselines: 20 easy, 20 medium, and 20 hard. The four baselines are (1) Dynamic Window Approach (DWA) [13]; (2) Timed Elastic Band (TEB) [14]; (3) end-to-end Reinforcement learning (RL) [15]; and Behavior Cloning (BC) [16]. The baselines' implementations are as follows:

a) Two Classical Local Planners: We employ two classical local planners: Dynamic Window Approach (DWA) [13] and Timed Elastic Band (TEB) [14]. These local planners are commonly used by the community due to their reliability in most navigation scenarios with open-sourced implementations that are integrated with the `move_base` navigation stack [40]. The hyper-parameters of the two local planners are manually tuned to improve their performances in the hard environments. Then, the hyper-parameters are fixed for all the experiments.

b) Behavior Cloning: The demonstration data is composed of 60 trajectories, with each collected from sixty dynamic environments, and another 60 trajectories collected from randomly sampled 300 BARN environments [10]. We learn a policy $\pi := S \rightarrow A$ to perform local motion planning. Here, S is the state space with each state $s \in S$ represented by a tuple (l, g_x, g_y) , where l is the 720-dim laser scan and

(g_x, g_y) are the x - y coordinates of the local goal location provided by Dijkstra’s global planner; A is the action space with each action $a = (v, w) \in A$, where $v \in [-0.5, 2]$ and $w \in [-3.14, 3.14]$ encode the linear and angular velocities of the robot respectively. The ranges of v and w are limited by the physical property of the Jackal robot. We represent such a policy by a multi-layer perceptron (MLP) neural network. The architecture of the neural network is shown in Fig. 4. More specifically, the 722-dimensional input is fed into a feature extraction network composed of three fully-connected layers with 512, 256, and 128 hidden units respectively. Then, the 128-dim feature embedding is fed into an actor network that connects a 64-hidden-unit layer and a 32-hidden-unit layer sequentially, and outputs a two-dimensional vector as the action. All the hidden layers are followed by the Tanh activation [41]. We collect one human-demonstrated trajectory from each of the 60 dynamic environments in DynaBARN and another one from each of the 60 randomly selected static environments in BARN [10].

c) Reinforcement Learning (RL): we also include a navigation policy learned from self-supervised reinforcement learning. More specifically, we employ Twin-delayed Deep Deterministic Policy Gradient (TD3) [15]. As one of the state-of-the-art off-policy RL algorithms, TD3 is relatively sample efficient and handles continuous actions by design. We use the same neural network (NN) architecture as the BC policy to represent the policy of the TD3 agent. As seen in Fig. 4 (bottom), to represent the critic network in the actor-critic framework, only the final layer of the actor network is modified to output the value prediction. To facilitate training, we also implement a parallelized training scheme that distributes multiple actors to a computing cluster to speed up the data collection process [30]. We train one navigation policy for 20 million time steps for each difficulty level with 20 training environments, and test them in the same environments they are trained on. To benchmark the

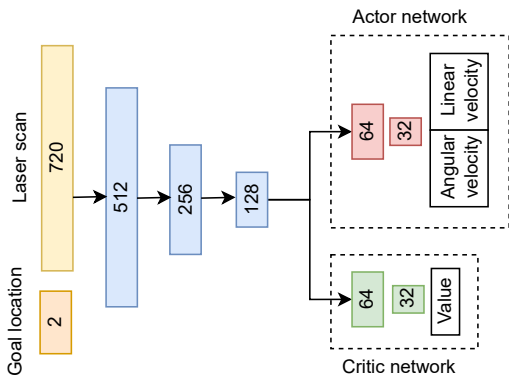


Fig. 4: The architectures of the actor and critic networks.

performances of the baselines, in each environment set with different difficulty levels (see Sec. III-C), we compare the average success rates of navigating in the environments. Since we care about the autonomous robot’s capability to navigate in a completely collision-free manner, the success

rate is the only metric we reported. Further metrics including traversal time and smoothness can be added for future research when the navigation systems are able to achieve very high success rates. The baselines are deployed in each environment 10 times to compute an average success rate. The average success rates in each environment set are reported in Fig. 5. The RL algorithm achieves the best overall performance, which is only slightly worse than DWA in the easy environments. This result is understandable since the RL agent has seen the largest amount of data points (20M) compared to other baselines. Between the classical local planners, DWA performs much better than TEB with about twice the success rates of TEB in easy and medium environments. Also, in hard environments, the success rate of TEB drops to almost zero, while DWA still maintains about 17%. Lastly, behavior cloning has the worst performance in all three difficulty levels, which reflects the difficulty of learning high-accuracy collision-avoidance behaviors from limited data.

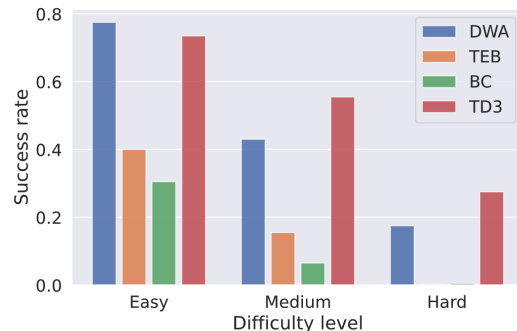


Fig. 5: Success rate of four baselines: DWA, TEB, TD3, and BC evaluated on easy, medium, and hard environments.

V. CONCLUSIONS

We present DynaBARN, a benchmark for autonomous robot navigation in dynamic environments where obstacles move according to a variety of different motion profiles. In order to test the robustness of autonomous navigation systems against different obstacle movement, we provide a systematic way to generate obstacle motion profiles and dynamic environments of different difficulties. We also provide a human demonstration data collection pipeline and the benchmarked performances of four different navigation systems as baselines. DynaBARN is developed to encourage further research on robust navigation in the presence of moving obstacles, including, and especially, the development of new, more robust algorithms than the baselines.

One limitation of the current version of DynaBARN is that all obstacles are cylindrical, which limits the navigation system’s robustness to obstacles with different shapes. One interesting extension to DynaBARN is to add randomized obstacle shapes. Another limitation is the lack of interaction between the obstacles and the robot: obstacles in the real world may or may not react to the obstacles, and if they do, they may react in different ways, e.g. yielding to the robot

earlier or later. Another future extension to DynaBARN is to add a variety of interaction types to the obstacles.

REFERENCES

- [1] J. Yu and S. M. LaValle, "Multi-agent path planning and network flow," in *Algorithmic foundations of robotics X*. Springer, 2013, pp. 157–173.
- [2] A. Gorbenko and V. Popov, "Multi-agent path planning," *Applied Mathematical Sciences*, vol. 6, no. 135, pp. 6733–6737, 2012.
- [3] D. Ferguson, M. Darms, C. Urmson, and S. Kolski, "Detection, prediction, and avoidance of dynamic obstacles in urban environments," in *2008 IEEE intelligent vehicles Symposium*. IEEE, 2008, pp. 1149–1154.
- [4] H.-U. Kobialka and V. Becanovic, "Speed-dependent obstacle avoidance by dynamic active regions," in *Robot Soccer World Cup*. Springer, 2003, pp. 534–542.
- [5] P. Long, T. Fan, X. Liao, W. Liu, H. Zhang, and J. Pan, "Towards optimally decentralized multi-robot collision avoidance via deep reinforcement learning," in *2018 IEEE International Conference on Robotics and Automation (ICRA)*. IEEE, 2018, pp. 6252–6259.
- [6] M. Everett, Y. F. Chen, and J. P. How, "Motion planning among dynamic, decision-making agents with deep reinforcement learning," in *2018 IEEE/RSJ International Conference on Intelligent Robots and Systems (IROS)*. IEEE, 2018, pp. 3052–3059.
- [7] G. Monaci, M. Aractingi, and T. Silander, "DiPCAN: Distilling privileged information for crowd-aware navigation," in *Robotics: Science and Systems (RSS) XVIII*, 2022.
- [8] H. Karnan, A. Nair, X. Xiao, G. Warnell, S. Pirk, A. Toshev, J. Hart, J. Biswas, and P. Stone, "Socially compliant navigation dataset (scand): A large-scale dataset of demonstrations for social navigation," *arXiv preprint arXiv:2203.15041*, 2022.
- [9] R. Mirsky, X. Xiao, J. Hart, and P. Stone, "Prevention and resolution of conflicts in social navigation—a survey," *arXiv preprint arXiv:2106.12113*, 2021.
- [10] D. Perille, A. Truong, X. Xiao, and P. Stone, "Benchmarking metric ground navigation," in *2020 IEEE International Symposium on Safety, Security, and Rescue Robotics (SSRR)*. IEEE, 2020, pp. 116–121.
- [11] D. Helbing and P. Molnar, "Social force model for pedestrian dynamics," *Physical review E*, vol. 51, no. 5, p. 4282, 1995.
- [12] J. Van Den Berg, S. J. Guy, M. Lin, and D. Manocha, "Optimal reciprocal collision avoidance for multi-agent navigation," in *Proc. of the IEEE International Conference on Robotics and Automation, Anchorage (AK), USA*, 2010.
- [13] D. Fox, W. Burgard, and S. Thrun, "The dynamic window approach to collision avoidance," *IEEE Robotics & Automation Magazine*, vol. 4, no. 1, pp. 23–33, 1997.
- [14] C. Rösmann, W. Feiten, T. Wösch, F. Hoffmann, and T. Bertram, "Trajectory modification considering dynamic constraints of autonomous robots," in *ROBOTIK 2012; 7th German Conference on Robotics*. VDE, 2012, pp. 1–6.
- [15] S. Fujimoto, H. van Hoof, and D. Meger, "Addressing function approximation error in actor-critic methods," 2018.
- [16] D. A. Pomerleau, "Alvin: An autonomous land vehicle in a neural network," *Advances in neural information processing systems*, vol. 1, 1988.
- [17] P. Fiorini and Z. Shiller, "Motion planning in dynamic environments using velocity obstacles," *The international journal of robotics research*, vol. 17, no. 7, pp. 760–772, 1998.
- [18] J. Van den Berg, M. Lin, and D. Manocha, "Reciprocal velocity obstacles for real-time multi-agent navigation," in *2008 IEEE international conference on robotics and automation*. IEEE, 2008, pp. 1928–1935.
- [19] X. Xiao, B. Liu, G. Warnell, and P. Stone, "Motion planning and control for mobile robot navigation using machine learning: a survey," *Autonomous Robots*, pp. 1–29, 2022.
- [20] Y. F. Chen, M. Liu, M. Everett, and J. P. How, "Decentralized non-communicating multiagent collision avoidance with deep reinforcement learning," in *2017 IEEE international conference on robotics and automation (ICRA)*. IEEE, 2017, pp. 285–292.
- [21] Y. F. Chen, M. Everett, M. Liu, and J. P. How, "Socially aware motion planning with deep reinforcement learning," in *2017 IEEE/RSJ International Conference on Intelligent Robots and Systems (IROS)*. IEEE, 2017, pp. 1343–1350.
- [22] L. Kästner, X. Zhao, T. Buiyan, J. Li, Z. Shen, J. Lambrecht, and C. Marx, "Connecting deep-reinforcement-learning-based obstacle avoidance with conventional global planners using waypoint generators," in *2021 IEEE/RSJ International Conference on Intelligent Robots and Systems (IROS)*. IEEE, 2021, pp. 1213–1220.
- [23] L. Kästner, B. Fatloun, Z. Shen, D. Gawrisch, and J. Lambrecht, "Human-following and-guiding in crowded environments using semantic deep-reinforcement-learning for mobile service robots," in *2022 International Conference on Robotics and Automation (ICRA)*. IEEE, 2022, pp. 833–839.
- [24] H. Kretzschmar, M. Spies, C. Sprunk, and W. Burgard, "Socially compliant mobile robot navigation via inverse reinforcement learning," *The International Journal of Robotics Research*, vol. 35, no. 11, pp. 1289–1307, 2016.
- [25] E. Heiden, L. Palmieri, L. Bruns, K. O. Arras, G. S. Sukhatme, and S. Koenig, "Bench-mr: A motion planning benchmark for wheeled mobile robots," *IEEE Robotics and Automation Letters*, vol. 6, no. 3, pp. 4536–4543, 2021.
- [26] I. A. Sucan, M. Moll, and L. E. Kavraki, "The open motion planning library," *IEEE Robotics & Automation Magazine*, vol. 19, no. 4, pp. 72–82, 2012.
- [27] X. Xiao, B. Liu, G. Warnell, J. Fink, and P. Stone, "Appld: Adaptive planner parameter learning from demonstration," *IEEE Robotics and Automation Letters*, vol. 5, no. 3, pp. 4541–4547, 2020.
- [28] Z. Wang, X. Xiao, B. Liu, G. Warnell, and P. Stone, "APPLI: Adaptive planner parameter learning from interventions," in *2021 IEEE International Conference on Robotics and Automation (ICRA)*. IEEE, 2021.
- [29] Z. Wang, X. Xiao, G. Warnell, and P. Stone, "APPLE: Adaptive planner parameter learning from evaluative feedback," in *2021 IEEE/RSJ International Conference on Intelligent Robots and Systems (IROS)*. IEEE, 2021.
- [30] Z. Xu, G. Dhamankar, A. Nair, X. Xiao, G. Warnell, B. Liu, Z. Wang, and P. Stone, "APPLR: Adaptive planner parameter learning from reinforcement," in *2021 IEEE International Conference on Robotics and Automation (ICRA)*. IEEE, 2021.
- [31] X. Xiao, Z. Wang, Z. Xu, B. Liu, G. Warnell, G. Dhamankar, A. Nair, and P. Stone, "Appl: Adaptive planner parameter learning," *Robotics and Autonomous Systems*, vol. 154, p. 104132, 2022.
- [32] X. Xiao, B. Liu, G. Warnell, and P. Stone, "Toward agile maneuvers in highly constrained spaces: Learning from hallucination," *IEEE Robotics and Automation Letters*, vol. 6, no. 2, pp. 1503–1510, 2021.
- [33] X. Xiao, B. Liu, and P. Stone, "Agile robot navigation through hallucinated learning and sober deployment," in *2021 IEEE International Conference on Robotics and Automation (ICRA)*. IEEE, 2021.
- [34] Z. Wang, X. Xiao, A. J. Nettekoven, K. Umasankar, A. Singh, S. Bommakanti, U. Topcu, and P. Stone, "From agile ground to aerial navigation: Learning from learned hallucination," in *2021 IEEE/RSJ International Conference on Intelligent Robots and Systems (IROS)*. IEEE, 2021.
- [35] C. Gloor, "Pedsim: Pedestrian crowd simulation," *URL http://pedsim.silmaril.org*, vol. 5, no. 1, 2016.
- [36] N. Tsoi, A. Xiang, P. Yu, S. S. Sohn, G. Schwartz, S. Ramesh, M. Hussein, A. W. Gupta, M. Kapadia, and M. Vázquez, "Sean 2.0: Formalizing and generating social situations for robot navigation," *IEEE Robotics and Automation Letters*, pp. 1–8, 2022.
- [37] L. Kastner, T. Bhuiyan, T. A. Le, E. Treis, J. Cox, B. Meinardus, J. Kmiecik, R. Carstens, D. Pichel, B. Fatloun, N. Khorsandi, and J. Lambrecht, "Arena-bench: A benchmarking suite for obstacle avoidance approaches in highly dynamic environments," *IEEE Robotics and Automation Letters*, pp. 1–8, 2022.
- [38] A. Biswas, A. Wang, G. Silvera, A. Steinfeld, and H. Admoni, "Socnavbench: A grounded simulation testing framework for evaluating social navigation," *ACM Transactions on Human-Robot Interaction (THRI)*, vol. 11, no. 3, pp. 1–24, 2022.
- [39] OSRF, "Ros wiki bags," <http://wiki.ros.org/Bags>, 2018.
- [40] "Ros wiki move_base," http://wiki.ros.org/move_base, 2018.
- [41] B. Karlik and A. V. Olgac, "Performance analysis of various activation functions in generalized mlp architectures of neural networks," *International Journal of Artificial Intelligence and Expert Systems*, vol. 1, no. 4, pp. 111–122, 2011.